

Dependence of the Glass Transition and Jamming Densities on Spatial Dimension

Monoj Adhikari,¹ Smarajit Karmakar,² and Srikanth Sastry^{3,*}

¹*Theoretical Sciences Unit, Jawaharlal Nehru Centre for Advanced Scientific Research,
Jakkur Campus, 560064 Bengaluru, India*

²*Tata Institute of Fundamental Research, 36/P, Gopanpally Village, Serilingampally Mandal, Ranga Reddy District,
Hyderabad 500046 Telangana, India*

³*Theoretical Sciences Unit and School of Advanced Materials, Jawaharlal Nehru Centre for Advanced Scientific Research,
Jakkur Campus, 560064 Bengaluru, India*

 (Received 6 April 2022; accepted 18 September 2023; published 18 October 2023)

We investigate the dynamics of soft sphere liquids through computer simulations for spatial dimensions from $d = 3$ to 8, over a wide range of temperatures and densities. Employing a scaling of density-temperature-dependent relaxation times, we precisely identify the density ϕ_0 , which marks the ideal glass transition in the hard sphere limit, and a crossover from sub- to super-Arrhenius temperature dependence. The difference between ϕ_0 and the athermal jamming density ϕ_J , small in 3 and 4 dimensions, increases with dimension, with $\phi_0 > \phi_J$ for $d > 4$. We compare our results with recent theoretical calculations.

DOI: [10.1103/PhysRevLett.131.168202](https://doi.org/10.1103/PhysRevLett.131.168202)

Introduction.—Fluid states of matter can transform to rigid, amorphous solids through the glass transition or the jamming transition. The glass transition describes the transition to disordered solid states typically in molecular systems upon a decrease in temperature, whose nature has been intensely investigated over several decades [1–5]. The jamming transition has likewise been widely investigated in *athermal* systems, typified by granular matter [6–8]. Their relationship has also been the subject of considerable research [9]. Whereas molecular glass formers and granular matter represent cases that exhibit one or the other of these phenomena, several systems, such as colloidal suspensions, in principle exhibit both phenomena, and their interplay is important, e.g., in their rheology [10]. Theoretical investigations over the last decade, extending the framework of the random first order transition theory [11–13], have focused on the hard sphere system in which both phenomena have been investigated in detail, and a unified mean-field description of both these phenomena has been developed in the limit of infinite dimensions [9,14–16]. These developments have naturally led to investigations of how the infinite-dimensional results relate to behavior in finite dimensions. An appealing and systematic approach to addressing questions in this regard is to study the effect of spatial dimensionality on the glass transition and jamming phenomenology, which have been pursued for hard particle systems extensively [9,16–23]. In addition to systems of hard spheres, a small number of other studies have investigated the role of dimensionality in determining aspects of glassy dynamics [24–28], such as dynamical heterogeneity in a binary mixture of the Lennard-Jones particles as a function of temperature. A more extensive investigation of the dependence on spatial dimensionality

in systems where both thermal and density effects play a role is thus of great interest. In this Letter, we study soft sphere assemblies interacting with a harmonic potential by investigating the dynamics at different densities and temperatures.

In the zero temperature limit, the behavior of this system approaches the density-controlled hard sphere model, while it is similar to thermally driven fluids at high density and finite temperature. In the athermal limit, the system *jams*, losing the ability to flow, at a critical density, ϕ_J , via the nonequilibrium jamming transition [29,30]. Several works [30–37] have considered and demonstrated the scenario that the jamming density is not unique, but can occur over a range of densities, above ϕ_J . In turn, the range of jamming densities is associated with a line of glass transition densities (kinetically determined or otherwise, as in mean-field results [9,15]) ending with a *Kauzmann* density ϕ_0 , which may be expected to be the relevant density for the divergence of relaxation times. The relationship between the jamming and Kauzmann densities have been investigated, with varying conclusions regarding the relative values of ϕ_J and ϕ_0 [17,38–42]. Several studies [9,16,34,41,43,44] also indicate that the relationship between these two transition densities depends on dimensionality.

In [39,40], the relaxation times were studied for the same model we consider in three dimensions. With increasing density, relaxation times exhibit a crossover from sub-Arrhenius to super-Arrhenius temperature dependence. Relaxation times were analyzed through a scaling function that assumes a divergence for the hard sphere systems at a density ϕ_0 , and by defining an effective hard sphere diameter at finite temperatures [45], to obtain two distinct

scaling collapses across ϕ_0 . The estimate of ϕ_0 thus obtained is very close to ϕ_J , the jamming point, although the meaning of the two densities was clearly distinguished.

Subsequently, the same scaling analysis was revisited in [46], where it was observed that good scaling collapse of comparable quality to [39,40] could be obtained for significantly different sets of parameter values ϕ_0 , δ and μ . Further, the parameters used to obtain scaling collapse [39,40] do not lead to an Arrhenius temperature dependence one may expect at $\phi = \phi_0$, as we explain below. To address these issues, we propose a new scaling analysis that ensures an Arrhenius temperature dependence at $\phi = \phi_0$, and employ a systematic procedure to estimate the density ϕ_0 reliably.

We perform extensive molecular dynamics simulations for a wide range of ϕ , T values in different spatial dimensions ranging from $d = 3$ to 8. We perform a scaling analysis similar to [39,40] but with a newly proposed scaling function to obtain ϕ_0 as a function of d . We obtain jamming densities following the analysis in [29,30]. Our results clearly demonstrate that $\phi_0 > \phi_J$ for $d > 4$, with ϕ_0/ϕ_J increasing with d , as may be expected from mean-field results [9,15,16].

Simulation details.—We study a 50:50 binary mixture of spheres of size ratio 1.4, interacting with a harmonic potential as a model glass former [47]:

$$V_{\alpha\beta}(r) = \frac{\epsilon_{\alpha\beta}}{2} \left(1 - \frac{r}{\sigma_{\alpha\beta}}\right)^2, \quad r_{\alpha\beta} \leq \sigma_{\alpha\beta}, \quad (1)$$

and $V_{\alpha\beta}(r) = 0$ for $r_{\alpha\beta} > \sigma_{\alpha\beta}$, where $\alpha, \beta \in (A, B)$, indicates the type of particle. Particle diameters σ_{AA} and σ_{BB} obey $\sigma_{BB}/\sigma_{AA} = 1.4$, and $\sigma_{AB} = (\sigma_{AA} + \sigma_{BB})/2$. The system size varies from 1000 to 5000 depending on the spatial dimension, with the linear extent of the simulated volume, $L > 2\sigma_{BB}$ in all dimensions. We investigate the dynamics at 10–14 densities (with 1–2 independent samples each) around the jamming density. The volume fraction, or density, $\phi = \rho V_d$, where $V_d = 2^{-d} \{\pi^{d/2} / \Gamma[1 + (d/2)]\} \times (c_A \sigma_{AA}^d + c_B \sigma_{BB}^d)$, $c_A = c_B = 1/2$, is the average volume per sphere in d dimensions, $\rho = (N/V)$ is the number density, N is the number of particles, and V is the volume. Molecular dynamics simulations are performed in a cubic box with the periodic boundary conditions, employing the constant temperature integration in [48], with time step $dt = 0.01$. Each independent run is of length $> 100\tau_\alpha$ where relaxation time τ_α , is computed from the overlap function $q(t)$ (for B particles) as $\langle q(t = \tau_\alpha) \rangle = 1/e$, with

$$q(t) = \frac{1}{N_B} \sum_{i=1}^{N_B} w(|\mathbf{r}_i(t_0) - \mathbf{r}_i(t + t_0)|), \quad (2)$$

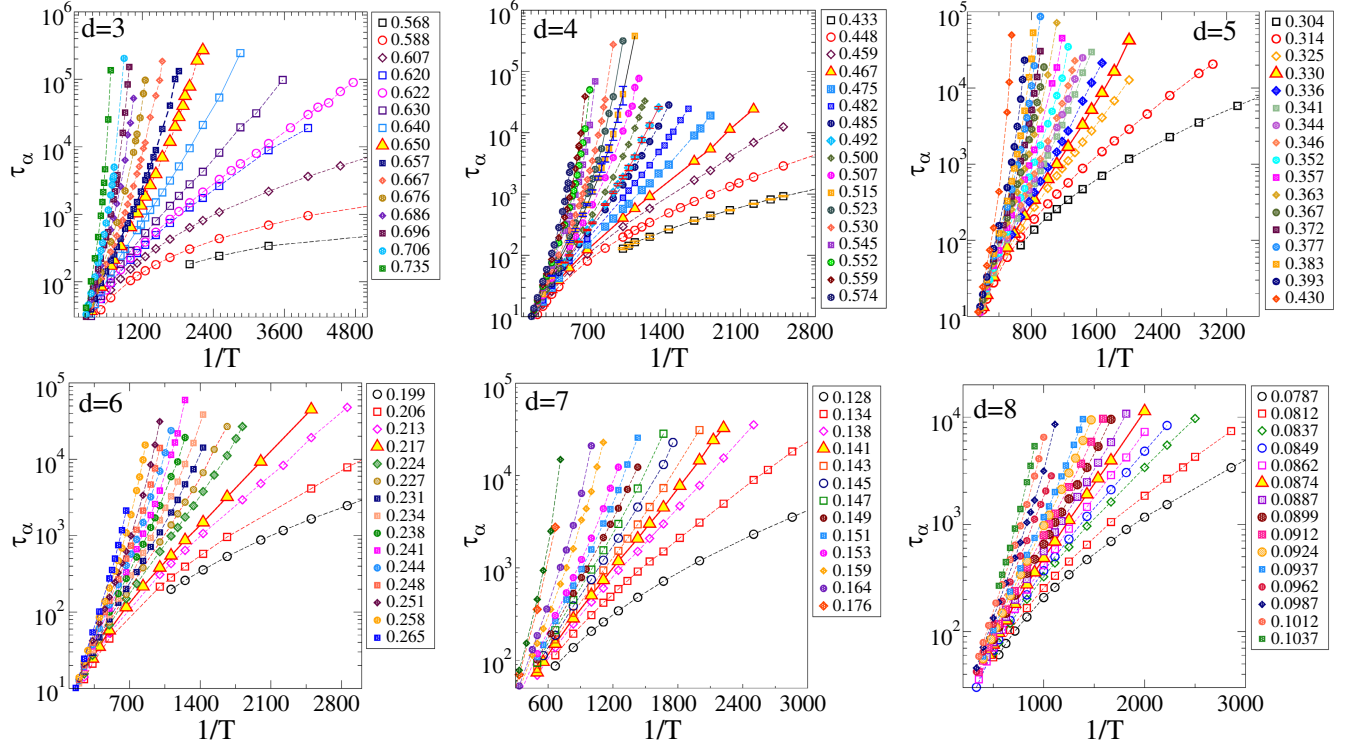


FIG. 1. Relaxation times as a function of inverse temperature are plotted in a semilog scale for several densities in different dimensions. Data shown with (yellow) filled triangles correspond to densities across which super-Arrhenius dependence is observed. Error bars (evaluated as standard deviations from independent estimates) are shown for selected densities for $d = 4$.

where $w(x) = 1$ if $x < a$ and 0 otherwise. The parameter “ a ” is chosen so that particle displacements from vibrational motion do not contribute to a reduction of overlap [49]. In Fig. 1, the relaxation time is plotted as a function of temperature for various densities for 3–8 dimensions. Additional details are provided in the Supplemental Material (SM) [50].

Results.—Considering an expression for relaxation times for hard sphere fluids of the form $\sqrt{T}\tau_\alpha^{\text{hs}} \sim \exp[A/(\phi_0 - \phi)^\delta]$, Berthier and Witten [39] analyzed relaxation times for soft spheres by defining a temperature-dependent effective volume fraction of the form $\phi_{\text{eff}} = \phi - aT^{\mu/2}$, which leads to the scaling form

$$\sqrt{T}\tau_\alpha(\phi, T) \sim \exp\left[\left(\frac{A}{|\phi_0 - \phi|^\delta}\right)F_\pm\left(\frac{|\phi_0 - \phi|^{\frac{2}{\mu}}}{T}\right)\right]. \quad (3)$$

$F_\pm(x)$ are unknown scaling functions that capture the distinct (super-Arrhenius, for $\phi > \phi_0$ and sub-Arrhenius, for $\phi < \phi_0$) temperature dependence of τ_α . Scaling collapse of $\tau_\alpha(\phi, T)$ is used to determine the parameters μ , δ , and ϕ_0 .

Plotting $|\phi_0 - \phi|^\delta \log(\sqrt{T}\tau_\alpha)$ against $|\phi_0 - \phi|^{(2/\mu)}/T$, with suitable choices of the parameters, a data collapse

on to two branches above and below ϕ_0 is obtained. The values of $\phi_0 = 0.635$ and $\delta = 2.2$ (in $d = 3$) were determined from such a procedure, with the δ value being in close agreement with experimental and simulation results for colloidal hard spheres and theoretical results [51–53]. The estimated ϕ_0 is close to but distinct from the jamming density of $\phi_J = 0.648$ estimated for the binary mixture studied in [29,30,39] and here.

The continuity of the functions F_+ and F_- in the scaling form in Eq. (3) suggests that $F_+(x) = F_-(x) \sim x^{\mu\delta/2}$ as $x \rightarrow 0$ (i.e., $\phi \rightarrow \phi_0$). Further, it is necessary to have $\mu\delta/2 = 1$ in order to obtain the expected Arrhenius form, $\tau \sim \exp(A/k_B T)$, at density ϕ_0 [as explained in the SM (S3.A)]. Imposing such a constraint, however, does not lead to the best data collapse [39], as we independently verify. It is thus desirable to explore alternate scaling functions, which we do in this work based on the evaluation of an effective diameter following the prescription in [54]. We compare our results to analysis employing Eq. (3), and obtain consistent estimates of ϕ_0 .

Following [54], the expression for the effective diameter with only temperature-dependent corrections can be written as $\sigma_{\text{eff}} = \int_0^\sigma [1 - \exp(-u(r)/k_B T)] dr$, leading to

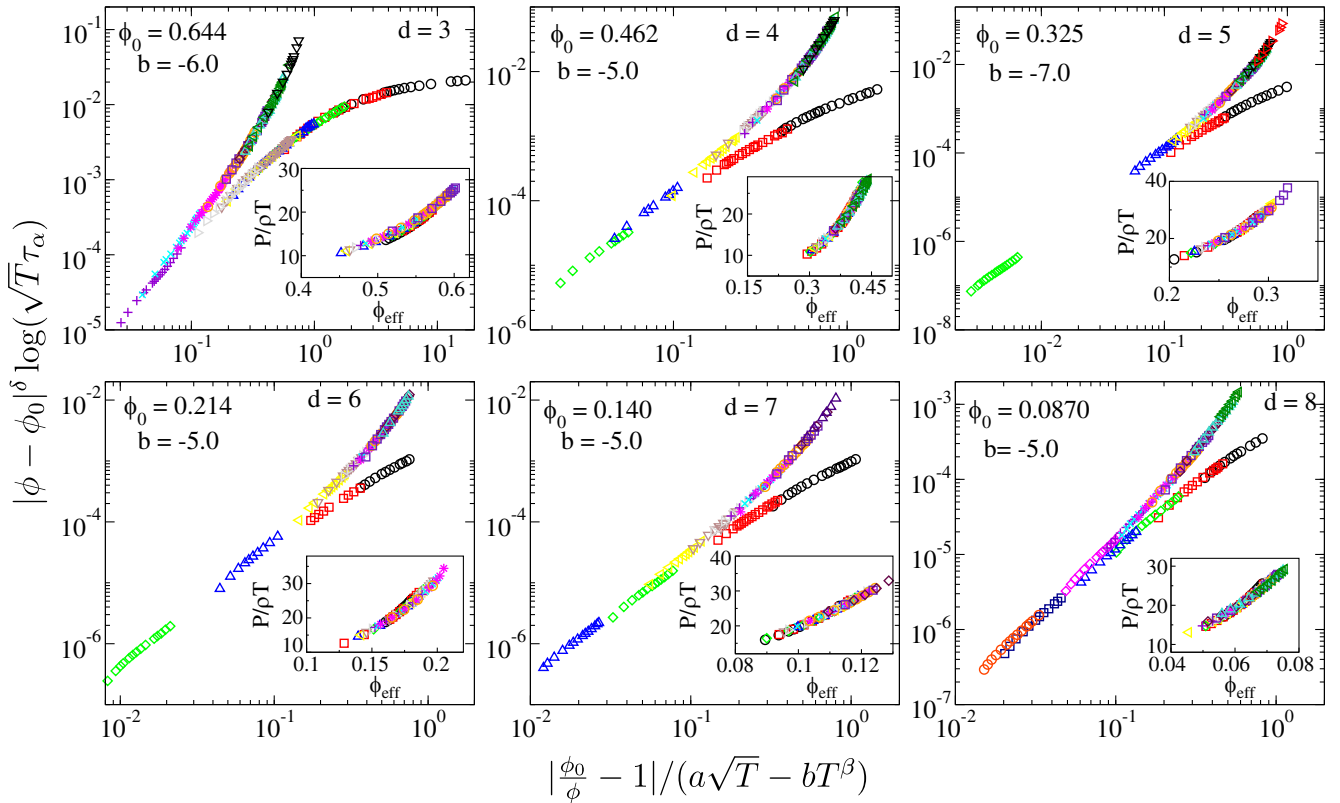


FIG. 2. Scaling plot of relaxation times for 3–8 spatial dimension. As explained in the text, coefficients a , b and exponent β describe the effective volume fraction ϕ_{eff} . Of these, we use fixed values of $a = d\sqrt{\pi}/2$ (see SM) and vary b , $\beta > 0.5$ to obtain collapse of pressures onto a single curve, $P/\rho T = f(\phi_{\text{eff}})$ (shown in the insets). Best data collapse is obtained around $\beta = 0.7$ (which we keep fixed), and the b values are indicated in the legends. Keeping $\delta = 2$ fixed, we vary ϕ_0 as the single fit parameter to obtain scaling plots of relaxation times τ_α shown.

$\sigma_{\text{eff}} \approx \sigma[1 - \frac{1}{2}\sqrt{\pi k_B T}]$, as explained in the SM (S3.B). In turn, the effective volume fraction in dimension d can be approximated as

$$\phi_{\text{eff}} \approx \phi \left(1 - a\sqrt{T} + bT^\beta\right), \quad (4)$$

where $a = d\sqrt{\pi}/2$, and the term bT^β approximates terms of $\mathcal{O}(T)$ and higher. Employing the effective ϕ in the expression for the hard sphere relaxation times, we write

$$\sqrt{T}\tau_\alpha(\phi, T) \sim \exp \left[\frac{A}{|\phi_0 - \phi|^\delta} F_\pm \left(\frac{|\frac{\phi_0}{\phi} - 1|}{a\sqrt{T} - bT^\beta} \right) \right]. \quad (5)$$

An Arrhenius form of the relaxation times at finite T and $\phi = \phi_0$ requires δ to be 2. The choice of $\delta = 2$, which we employ, is justified by the analysis provided in the SM (S5.A). Rather than estimate b , β , and ϕ_0 through a scaling analysis of τ_α , we first require that $P/\rho T$ where P is the pressure is a unique function of ϕ_{eff} and estimate b and β from the data collapse of $P/\rho T$ (shown in the insets of Fig. 2). Scaling collapse of τ_α through Eq. (5), shown in Fig. 2, is used to estimate the remaining parameter ϕ_0 . Additional details regarding the data collapse procedure including error analysis are provided in the SM.

We next estimate the jamming densities following the protocol employed in [30], wherein initially random configurations are compressed till the energy reaches 10^{-5} , and decompressed till the energy decreases below 10^{-16} , at the jamming density (see SM for additional details). Figure 3(a) illustrates the protocol for $d = 5$ (corresponding data for all dimensions are shown in the SM). Based on the initial configuration used, the ϕ_J we estimate corresponds to the low density limit of the range over which jamming can take place [29,30]. The procedure is applied to 1000 independent initial configurations, and the histogram of jamming densities obtained is shown in Fig. 3(b). The average jamming density ϕ_J is shown in Fig. 3(c) (also tabulated in Table I), along with estimates of ϕ_0 obtained above. The ratio ϕ_0/ϕ_J , shown in the inset, increases with d , with $\phi_0 > \phi_J$ for $d > 4$, whereas for $d = 3, 4$, $\phi_0 < \phi_J$, with the two values being very close. The jamming densities ϕ_J we obtain are very similar to, but slightly larger than, those obtained for monodisperse spheres in [21,55]. In Fig. 3(d), we compare the scaled jamming densities we obtain with those in [55]. We also show the recent theoretical calculations in [16] for the corresponding quantity ϕ_{th} , which shows the same trend as our ϕ_J data, but are smaller. There is no accurate theoretical prediction for ϕ_J for reasons discussed in Ref. [56], and the ϕ_{th} values computed in [16] can only be used as rough estimates, which underestimate our results of ϕ_J as well as those in [21,55]. We further show the ϕ_0 values we obtain, along with the corresponding calculated values (Kauzmann density ϕ_K) in [16]. Although we are not

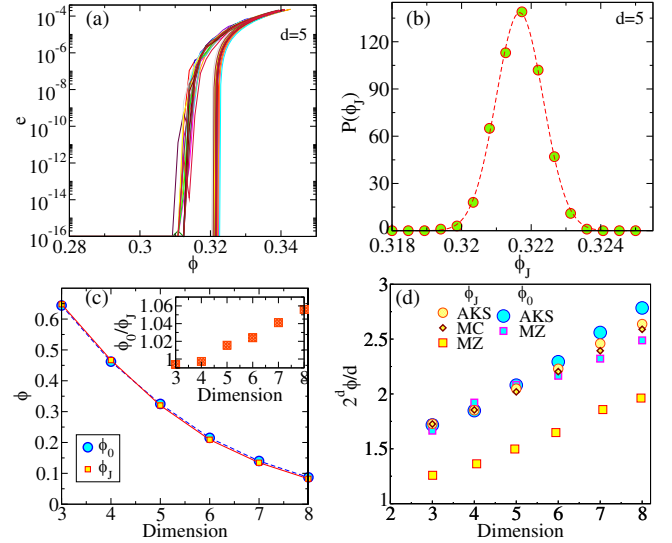


FIG. 3. (a) The energies during compression-decompression cycles of energy-minimized configurations plotted as a function of volume fraction for $d = 5$. Data are shown for 50 independent samples. (b) The histogram of jamming densities for $d = 5$. (c) The jamming density, ϕ_J , and the glass transition density, ϕ_0 , plotted as a function of spatial dimension. Inset: ratio of ϕ_0 and ϕ_J , plotted as a function of spatial dimension. (d) Comparison of ϕ_0 and ϕ_J values from the present work (AKS) with previous simulation [55] (MC) and theoretical calculations [16] (MZ) using the Percus-Yevick closure.

able to verify quantitatively the prediction that ϕ_0 increases as $\log d$ [15,16], we note that the values of ϕ_0 calculated in [16] are in near quantitative agreement with our results.

Finally, we compute the temperature at which the relaxation times show an apparent divergence by fitting the data at each density above ϕ_0 , for each dimension, to the Vogel-Fulcher-Tammann (VFT) form, $\tau_\alpha = \tau_0 \exp \{1/K_{\text{VFT}}[(T/T_{\text{VFT}}) - 1]\}$. In Fig. 4, we show the density-temperature diagram for $d = 3$ and $d = 7$

TABLE I. Jamming and glass transition densities ϕ_J and ϕ_0 for dimensions d from 3 to 8. Error bars for ϕ_0 are obtained by considering an increase in the error χ^2_τ (defined in SM) by 20% of the lowest value. The error bars of ϕ_J are computed from half width at half maximum of the distribution of ϕ_J [shown Fig. 3(b) and the SM]. For comparison, we have shown theoretical values ϕ_0 values from Ref. [16].

D	ϕ_J (AKS)	ϕ_0 (AKS)	ϕ_0 (MZ [16])
3	0.648 ± 0.0014	0.644 ± 0.003	0.624414
4	0.467 ± 0.0015	0.462 ± 0.004	0.480302
5	0.320 ± 0.0008	0.325 ± 0.003	0.325298
6	0.209 ± 0.0006	0.214 ± 0.002	0.203008
7	0.1345 ± 0.0004	0.140 ± 0.002	0.126974
8	0.0824 ± 0.0003	0.0870 ± 0.001	0.0777626

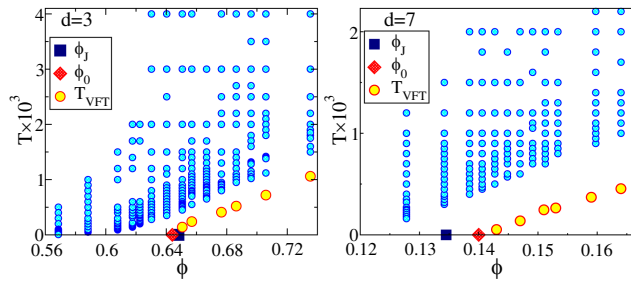


FIG. 4. The jamming and glass transition densities ϕ_J (navy blue square) and ϕ_0 (red diamond) are shown for $d = 3$ and $d = 7$ along with the density-dependent glass transition temperatures T_{VFT} (orange circles), and the set of densities and temperatures at which simulations have been performed (blue circles).

(results for other dimensions are shown in the SM), which shows ϕ_0 and ϕ_J along with the density dependent T_{VFT} . The results shown illustrate the manner in which the relationship between ϕ_0 and ϕ_J changes with spatial dimension. The T_{VFT} values shown extrapolate to zero at $\phi \rightarrow \phi_0$, illustrating that ϕ_0 is the relevant limit density for the density-dependent glass transition.

Conclusion.—To summarize, we have studied the dynamics of model glass forming liquids consisting of soft (harmonic) spheres by measuring relaxation times as a function of temperature for several densities for spatial dimensions 3–8. The temperature dependence exhibits a crossover from sub-Arrhenius to super-Arrhenius behavior as density increases. We perform a new scaling analysis of the relaxation times to identify a density ϕ_0 , which corresponds to the ideal glass transition density for the hard sphere (or zero temperature) limit. We also estimate the (lowest) jamming density ϕ_J , and show that for $d > 4$, $\phi_0 > \phi_J$, which clearly demonstrates that the jamming and glass transitions are distinct in all dimensions. Comparing with theoretical calculations in [16], we find near quantitative agreement with our estimated ϕ_0 values (albeit with a steeper d dependence for the ϕ_0 we obtain), whereas the ϕ_J values we obtain are underestimated by the ϕ_{ih} computed in [16], the reasons for which are discussed in [56]. Our results thus provide a useful benchmark for future efforts in developing quantitative theories of the glass and jamming transitions.

We thank Francesco Zamponi, Patrick Charbonneau, and Peter Morse for useful discussions, sharing results, and comments on the manuscript. We gratefully acknowledge Anshul Parmar for significant help in setting up the numerical investigations presented in this Letter. We acknowledge the Thematic Unit of Excellence on Computational Materials Science, and the National Supercomputing Mission facility (Param Yukti) at the Jawaharlal Nehru Center for Advanced Scientific Research for computational resources. S. K. acknowledges

support from Swarna Jayanti Fellowship Grants No. DST/SJF/PSA-01/2018-19 and No. SB/SFJ/2019-20/05. S. S. acknowledges support through the JC Bose Fellowship (JBR/2020/000015) SERB, DST (India).

*Corresponding author: sastry@jncasr.ac.in

- [1] P. G. Debenedetti and F. H. Stillinger, *Nature (London)* **410**, 259 (2001).
- [2] K. Binder and W. Kob, *Glassy Materials and Disordered Solids: An Introduction to Their Statistical Mechanics* (World scientific, Singapore, 2011).
- [3] L. Berthier and G. Biroli, *Rev. Mod. Phys.* **83**, 587 (2011).
- [4] S. Karmakar, C. Dasgupta, and S. Sastry, *Annu. Rev. Condens. Matter Phys.* **5**, 255 (2014).
- [5] C. P. Royall, F. Turci, S. Tatsumi, J. Russo, and J. Robinson, *J. Phys. Condens. Matter* **30**, 363001 (2018).
- [6] A. J. Liu and S. R. Nagel, *Annu. Rev. Condens. Matter Phys.* **1**, 347 (2010).
- [7] S. Torquato and F. H. Stillinger, *Rev. Mod. Phys.* **82**, 3197 (2010).
- [8] R. P. Behringer and B. Chakraborty, *Rep. Prog. Phys.* **82**, 012601 (2018).
- [9] P. Charbonneau, J. Kurchan, G. Parisi, P. Urbani, and F. Zamponi, *Annu. Rev. Condens. Matter Phys.* **8**, 265 (2017).
- [10] A. Ikeda, L. Berthier, and P. Sollich, *Phys. Rev. Lett.* **109**, 018301 (2012).
- [11] T. R. Kirkpatrick and D. Thirumalai, *Phys. Rev. Lett.* **58**, 2091 (1987).
- [12] T. R. Kirkpatrick and D. Thirumalai, *Phys. Rev. A* **37**, 4439 (1988).
- [13] T. R. Kirkpatrick, D. Thirumalai, and P. G. Wolynes, *Phys. Rev. A* **40**, 1045 (1989).
- [14] T. R. Kirkpatrick and P. Wolynes, *Phys. Rev. A* **35**, 3072 (1987).
- [15] G. Parisi, P. Urbani, and F. Zamponi, *Theory of Simple Glasses: Exact Solutions in Infinite Dimensions* (Cambridge University Press, Cambridge, England, 2020).
- [16] M. Mangeat and F. Zamponi, *Phys. Rev. E* **93**, 012609 (2016).
- [17] P. Charbonneau, A. Ikeda, G. Parisi, and F. Zamponi, *Phys. Rev. Lett.* **107**, 185702 (2011).
- [18] P. Charbonneau, A. Ikeda, G. Parisi, and F. Zamponi, *Proc. Natl. Acad. Sci. U.S.A.* **109**, 13939 (2012).
- [19] B. Charbonneau, P. Charbonneau, Y. Jin, G. Parisi, and F. Zamponi, *J. Chem. Phys.* **139**, 164502 (2013).
- [20] L. Berthier, P. Charbonneau, and J. Kundu, *Phys. Rev. Lett.* **125**, 108001 (2020).
- [21] P. Charbonneau and P. K. Morse, *Phys. Rev. Lett.* **126**, 088001 (2021).
- [22] A. Zacccone, *Phys. Rev. Lett.* **128**, 028002 (2022).
- [23] P. Charbonneau and P. K. Morse, [arXiv:2201.07629](https://arxiv.org/abs/2201.07629).
- [24] J. D. Eaves and D. R. Reichman, *Proc. Natl. Acad. Sci. U.S.A.* **106**, 15171 (2009).
- [25] S. Sengupta, S. Karmakar, C. Dasgupta, and S. Sastry, *Phys. Rev. Lett.* **109**, 095705 (2012).
- [26] S. Sengupta, S. Karmakar, C. Dasgupta, and S. Sastry, *J. Chem. Phys.* **138**, 12A548 (2013).

- [27] W.-S. Xu, J. F. Douglas, and K. F. Freed, *Adv. Chem. Phys.* **161**, 443 (2016).
- [28] M. Adhikari, S. Karmakar, and S. Sastry, *J. Phys. Chem. B* **125**, 10232 (2021).
- [29] C. S. O'Hern, L. E. Silbert, A. J. Liu, and S. R. Nagel, *Phys. Rev. E* **68**, 011306 (2003).
- [30] P. Chaudhuri, L. Berthier, and S. Sastry, *Phys. Rev. Lett.* **104**, 165701 (2010).
- [31] R. J. Speedy, *J. Phys. Condens. Matter* **10**, 4185 (1998).
- [32] R. J. Speedy and P. G. Debenedetti, *Mol. Phys.* **88**, 1293 (1996).
- [33] F. Krzakala and J. Kurchan, *Phys. Rev. E* **76**, 021122 (2007).
- [34] R. Mari, F. Krzakala, and J. Kurchan, *Phys. Rev. Lett.* **103**, 025701 (2009).
- [35] M. Hermes and M. Dijkstra, *Europhys. Lett.* **89**, 38005 (2010).
- [36] M. Ciamarra, A. Coniglio, and A. D. Candia, *Soft Matter* **6**, 2975 (2010).
- [37] M. Ozawa, T. Kuroiwa, A. Ikeda, and K. Miyazaki, *Phys. Rev. Lett.* **109**, 205701 (2012).
- [38] R. D. Kamien and A. J. Liu, *Phys. Rev. Lett.* **99**, 155501 (2007).
- [39] L. Berthier and T. A. Witten, *Europhys. Lett.* **86**, 10001 (2009).
- [40] L. Berthier and T. A. Witten, *Phys. Rev. E* **80**, 021502 (2009).
- [41] A. Coniglio, M. P. Ciamarra, and T. Aste, *Soft Matter* **13**, 8766 (2017).
- [42] L. Berthier, D. Coslovich, A. Ninarello, and M. Ozawa, *Phys. Rev. Lett.* **116**, 238002 (2016).
- [43] M. P. Ciamarra, M. Nicodemi, and A. Coniglio, *Soft Matter* **6**, 2871 (2010).
- [44] J. Kurchan, G. Parisi, P. Urbani, and F. Zamponi, *J. Phys. Chem. B* **117**, 12979 (2013).
- [45] M. H. Cohen and D. Turnbull, *J. Chem. Phys.* **31**, 1164 (1959).
- [46] M. Maiti and M. Schmiedeberg, *J. Phys. Condens. Matter* **31**, 165101 (2019).
- [47] D. J. Durian, *Phys. Rev. Lett.* **75**, 4780 (1995).
- [48] D. Brown and J. Clarke, *Mol. Phys.* **51**, 1243 (1984).
- [49] N. Lačević, F. W. Starr, T. Schröder, and S. Glotzer, *J. Chem. Phys.* **119**, 7372 (2003).
- [50] See Supplemental Material at <http://link.aps.org/supplemental/10.1103/PhysRevLett.131.168202>, which contains a description of the procedure used to define the overlap function, the scaling analysis using the scaling function defined by Berthier and Witten, the new effective diameter definition we employ in this work and the corresponding scaling function, comparison of results from the Berthier-Witten scaling function and the one proposed in this work, error analysis for different data collapse procedures employed, details of the procedure used for obtaining jamming densities, comparison of jamming densities obtained with previous work, the density-temperature phase diagram for all the dimensions investigated, and the statistics of rattlers.
- [51] R. W. Hall and P. G. Wolynes, *J. Chem. Phys.* **86**, 2943 (1987).
- [52] G. Brambilla, D. El Masri, M. Pierno, L. Berthier, L. Cipelletti, G. Petekidis, and A. B. Schofield, *Phys. Rev. Lett.* **102**, 085703 (2009).
- [53] V. Baranau and U. Tallarek, *AIP Adv.* **10**, 035212 (2020).
- [54] J. A. Barker and D. Henderson, *J. Chem. Phys.* **47**, 4714 (1967).
- [55] P. K. Morse and E. I. Corwin, *Phys. Rev. Lett.* **112**, 115701 (2014).
- [56] A. Manacorda and F. Zamponi, *J. Phys. A* **55**, 334001 (2022).